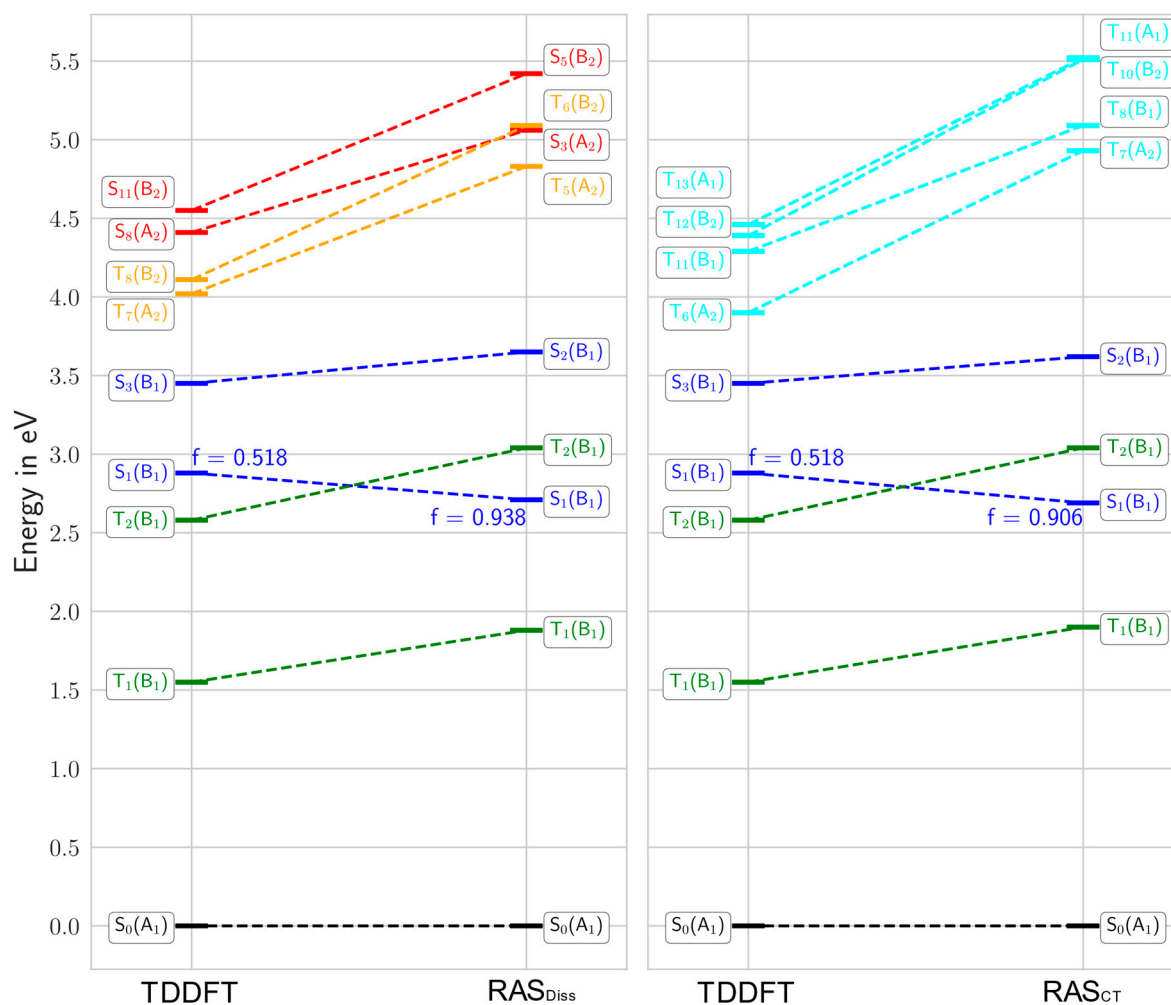# Supplementary Materials: Photo-induced Charge Separation vs. Degradation of a BODIPY-Based Photosensitizer Assessed by TDDFT and RASPT2

Karl Michael Ziems, Stefanie Gräfe and Stephan Kupfer *

1. Preliminary benchmark

Figure S1. Comparison of TDDFT and MS-RASPT2 at GS S_0 geometry $^1\mathbf{1}^0$ for the non-reduced dye. Left: comparison for dissociative states with RAS_{Diss}. Right: comparison for CT states with RAS_{CT}. Colour code: singlet ground state (black), excited singlet state (blue), dissociative singlet state (red), triplet state (green), dissociative triplet state (orange), triplet CT state (cyan).
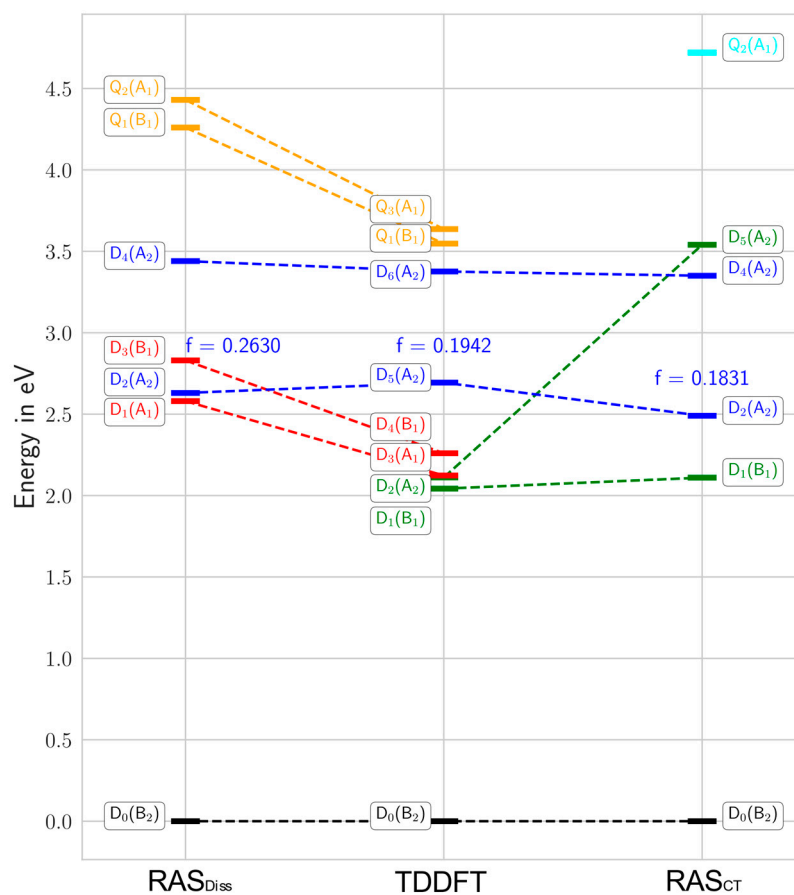
Figure S2. Comparison of TDDFT and MS-RASPT2 (RAS$_{Diss}$ and RAS$_{CT}$) states at singly reduced GS D$_0$ geometry ^{2}**1**$^{-1}$. Colour code: doublet ground state (black), excited doublet state (blue), dissociative doublet state (red), CT doublet state (green), dissociative quartet state (orange), CT quartet state (cyan).

Table S1. TDDFT calculated vertical excitation energies (E), wavelengths (λ), oscillator strengths (f), and singly-excited configurations of the main excited singlet-singlet and singlet-triplet transitions involved in the initial absorption of $^1\mathbf{1^0}$ within the Franck-Condon region.

	Transition	Weight / %	E / eV	λ / nm	f	Character
S_0 (A_1)	HF	-	-	-	-	HF
S_1 (B_1)	$\pi_3(a_2) \rightarrow \pi_4^*(b_2)$	89	2.88	430	0.5183	HOMO $\rightarrow$ LUMO
	$\pi_2(a_2) \rightarrow \pi_4^*(b_2)$	11				HOMO-1 $\rightarrow$ LUMO
S_2 (A_1)	$\pi_2(b_2) \rightarrow \pi_4^*(b_2)$	98	3.44	360	0.0454	
S_3 (B_1)	$\pi_2(a_2) \rightarrow \pi_4^*(b_2)$	88	3.45	359	0.3113	HOMO-1 $\rightarrow$ LUMO
	$\pi_3(a_2) \rightarrow \pi_4^*(b_2)$	12				HOMO $\rightarrow$ LUMO
S_8 (A_2)	$\pi_3(a_2) \rightarrow \sigma^*(a_1)$	93	4.41	281	0.0000	Diss
S_{11} (B_2)	$\pi_3(a_2) \rightarrow \sigma^*(b_1)$	87	4.55	272	0.0001	Diss
T_1 (B_1)	$\pi_3(a_2) \rightarrow \pi_4^*(b_2)$	96	1.55	800	-	HOMO $\rightarrow$ LUMO
T_2 (B_1)	$\pi_2(a_2) \rightarrow \pi_4^*(b_2)$	89	2.58	480	-	HOMO-1 $\rightarrow$ LUMO
T_3 (A_1)	$\pi_2(b_2) \rightarrow \pi_4^*(b_2)$	90	2.75	451	-	
T_4 (A_1)	$\pi_3(b_2) \rightarrow \pi_4^*(b_2)$	80	3.36	369	-	
	$p(b_2) \rightarrow \pi_4^*(b_2)$	12				
T_6 (A_2)	$\pi_{ph,2}(b_1) \rightarrow \pi_4^*(b_2)$	82	3.90	318	-	CT
T_7 (A_2)	$\pi_3(a_2) \rightarrow \sigma^*(a_1)$	70	4.02	308	-	Diss
	$\pi_2(b_2) \rightarrow \sigma^*(b_1)$	17				
	$\pi_2(a_2) \rightarrow \sigma^*(a_1)$	10				
T_8 (B_2)	$\pi_3(a_2) \rightarrow \sigma^*(b_1)$	58	4.11	302	-	Diss
	$\pi_2(b_2) \rightarrow \sigma^*(a_1)$	26				
	$\pi_2(a_2) \rightarrow \sigma^*(b_1)$	11				
T_{11} (B_1)	$\pi_{ph,3}(a_2) \rightarrow \pi_4^*(b_2)$	100	4.29	289	-	CT
T_{12} (B_2)	$\pi_3(a_2) \rightarrow \pi_{ph,5}^*(b_1)$	94	4.39	282	-	CT
T_{13} (A_1)	$\pi_3(a_2) \rightarrow \pi_{ph,4}^*(a_2)$	85	4.46	278	-	CT

Table S2. Vertical excitation energies (E), wavelengths (λ), oscillator strengths (f), and singly-excited configurations of the main excited singlet-singlet and singlet-triplet transitions involved in the initial absorption of $^1\mathbf{1}^0$ within the Franck-Condon region. Calculated at the MS-RASPT2 level of theory using RAS$_{Diss}$ and a level shift of 0.3 a.u. Double excitations are indicated by DE.

	Transition	Weight / %	E / eV	λ / nm	f	Character
S_0 (A_1)	-	83	-	-	-	HF
S_1 (B_1)	$\pi_3(a_2) \rightarrow \pi_4^*(b_2)$	76	2.71	457	0.9383	HOMO $\rightarrow$ LUMO
S_2 (B_1)	$\pi_2(a_2) \rightarrow \pi_4^*(b_2)$	75	3.65	340	0.0939	HOMO-1 $\rightarrow$ LUMO
S_3 (A_2)	$\pi_3(a_2) \rightarrow \sigma^*(a_1)$	74	5.06	245	0.0000	Diss
S_4 (A_1)	DE: $\pi_3(a_2) \rightarrow \pi_4^*(b_2)$	59	5.06	245	0.0030	HOMO $\rightarrow$ LUMO
	$\pi_3(b_2) \rightarrow \pi_4^*(b_2)$	13				
S_5 (B_2)	$\pi_3(a_2) \rightarrow \sigma^*(b_1)$	77	5.52	229	0.0012	Diss
S_6 (A_2)	$\pi_{ph,2}(b_1) \rightarrow \pi_4^*(b_2)$	86	5.91	210	0.0000	CT
S_7 (A_2)	$\pi_2(a_2) \rightarrow \sigma^*(a_1)$	64	5.93	209	0.0000	Diss
S_8 (B_2)	$\pi_3(a_2) \rightarrow \pi_{ph,5}^*(b_1)$	84	6.33	196	0.0000	CT
T_1 (B_1)	$\pi_3(a_2) \rightarrow \pi_4^*(b_2)$	82	1.88	658	-	HOMO $\rightarrow$ LUMO
T_2 (B_1)	$\pi_2(a_2) \rightarrow \pi_4^*(b_2)$	78	3.04	408	-	HOMO-1 $\rightarrow$ LUMO
T_3 (A_1)	$\pi_2(b_2) \rightarrow \pi_4^*(b_2)$	47	4.09	303	-	
	$\pi_3(b_2) \rightarrow \pi_4^*(b_2)$	24				
T_4 (A_1)	$\pi_3(b_2) \rightarrow \pi_4^*(b_2)$	49	4.78	260	-	
	$\pi_2(b_2) \rightarrow \pi_4^*(b_2)$	24				
T_5 (A_2)	$\pi_3(a_2) \rightarrow \sigma^*(a_1)$	72	4.83	257	-	Diss
T_6 (B_2)	$\pi_3(a_2) \rightarrow \sigma^*(b_1)$	60	5.09	244	-	Diss
	$\pi_2(a_2) \rightarrow \sigma^*(b_1)$	14				
T_7 (A_2)	$\pi_2(a_2) \rightarrow \sigma^*(a_1)$	62	5.83	213	-	Diss
T_8 (A_2)	$\pi_{ph,2}(b_1) \rightarrow \pi_4^*(b_2)$	86	5.95	208	-	CT
T_9 (B_2)	$\pi_2(a_2) \rightarrow \sigma^*(b_1)$	49	5.99	207	-	Diss
	$\pi_3(a_2) \rightarrow \sigma^*(b_1)$	16				

Table S3. Vertical excitation energies (E), wavelengths (λ), oscillator strengths (f), and singly-excited configurations of the main excited singlet-singlet and singlet-triplet transitions involved in the initial absorption of $^1\mathbf{1^0}$ within the Franck-Condon region. Calculated at the MS-RASPT2 level of theory using RAS$_{CT}$ and a level shift of 0.3 a.u.

	Transition	Weight / %	E / eV	λ / nm	f	Character
S_0 (A_1)	-	79	-	-	-	HF
S_1 (B_1)	$\pi_3(a_2) \rightarrow \pi_4^*(b_2)$	73	2.69	460	0.9059	HOMO $\rightarrow$ LUMO
S_2 (B_1)	$\pi_2(a_2) \rightarrow \pi_4^*(b_2)$	68	3.62	342	0.0987	HOMO-1 $\rightarrow$ LUMO
S_3 (A_1)	$\pi_2(b_2) \rightarrow \pi_4^*(b_2)$	53	4.52	275	0.0562	
	DE: $\pi_3(a_2) \rightarrow \pi_4^*(b_2)$	17				HOMO $\rightarrow$ LUMO
T_1 (B_1)	$\pi_3(a_2) \rightarrow \pi_4^*(b_2)$	72	1.90	654	-	HOMO $\rightarrow$ LUMO
T_2 (B_1)	$\pi_2(a_2) \rightarrow \pi_4^*(b_2)$	75	3.04	408	-	HOMO-1 $\rightarrow$ LUMO
T_3 (A_1)	$\pi_2(b_2) \rightarrow \pi_4^*(b_2)$	64	4.16	298	-	
T_4 (A_1)	$\pi_{ph,3}(a_2) \rightarrow \pi_{ph,4}^*(a_2)$	40	4.45	279	-	Intra Ph
	$\pi_{ph,2}(b_1) \rightarrow \pi_{ph,5}^*(b_1)$	31				
T_5 (B_2)	$\pi_{ph,3}(a_2) \rightarrow \pi_{ph,5}^*(b_1)$	39	4.84	256	-	Intra Ph
	$\pi_{ph,2}(b_1) \rightarrow \pi_{ph,4}^*(a_2)$	36				
T_6 (A_1)	$\pi_3(b_2) \rightarrow \pi_4^*(b_2)$	65	4.85	256	-	
T_7 (A_2)	$\pi_{ph,2}(b_1) \rightarrow \pi_4^*(b_2)$	81	4.93	252	-	CT
T_8 (B_1)	$\pi_{ph,3}(a_2) \rightarrow \pi_4^*(b_2)$	72	5.09	243	-	CT
T_9 (A_1)	$\pi_{ph,2}(b_1) \rightarrow \pi_{ph,5}^*(b_1)$	43	5.23	237	-	Intra Ph
	$\pi_{ph,3}(a_2) \rightarrow \pi_{ph,4}^*(a_2)$	21				
T_{10} (B_2)	$\pi_3(a_2) \rightarrow \pi_{ph,5}^*(b_1)$	68	5.51	225	-	CT
T_{11} (A_1)	$\pi_3(a_2) \rightarrow \pi_{ph,4}^*(a_2)$	68	5.52	225	-	CT
T_{12} (A_2)	$\pi_3(a_2) \rightarrow \sigma^*(a_1)$	42	5.54	224	-	Diss
	$\pi_2(a_2) \rightarrow \sigma^*(a_1)$	50				
	$\pi_2(b_2) \rightarrow \sigma^*(b_1)$	15				
T_{13} (B_2)	$\pi_2(a_2) \rightarrow \sigma^*(b_1)$	56	5.82	213	-	Diss
	$\pi_2(b_2) \rightarrow \sigma^*(a_1)$	11				

Table S4. TDDFT calculated vertical excitation energies (E), wavelengths (λ), oscillator strengths (f), spin ($2S + 1$) and singly-excited configurations of the main excited doublet-doublet and doublet-quartet transitions involved in the initial absorption of $^2\mathbf{1}^{-1}$ within the Franck-Condon region.

	Transition	Weight / %	E / eV	λ / nm	f	Spin	Character
D_0 (B_2)	HF	-	-	-	-	2.02	HF
D_1 (B_1)	$\pi_4^*(b_2) \rightarrow \pi_{ph,5}^*(b_1)$	99	2.04	607	0.0000	2.03	
D_2 (A_2)	$\pi_4^*(b_2) \rightarrow \pi_{ph,4}^*(a_2)$	98	2.11	587	0.0000	2.03	
D_3 (A_1)	$\pi_4^*(b_2) \rightarrow \sigma^*(a_1)$	95	2.12	584	0.0000	2.11	
D_4 (B_1)	$\pi_4^*(b_2) \rightarrow \sigma^*(b_1)$	94	2.26	549	0.0000	2.12	
D_5 (A_2)	$\pi_3(a_2) \rightarrow \pi_4^*(b_2)$	87	2.69	460	0.1942	2.05	HOMO $\rightarrow$ LUMO
D_6 (A_2)	$\pi_2(a_2) \rightarrow \pi_4^*(b_2)$	93	3.38	367	0.0034	2.08	HOMO-1 $\rightarrow$ LUMO
Q_1 (B_1)	$\pi_3(a_2) \rightarrow \sigma^*(a_1)$	60	3.55	350	-	3.25	Diss
	$\pi_2(a_2) \rightarrow \sigma^*(a_1)$	10					
Q_2 (B_2)	$\pi_{ph,2}(b_1) \rightarrow \pi_{ph,5}^*(b_1)$	52	3.62	342	-	3.46	Intra Ph
	$\pi_{ph,3}(a_2) \rightarrow \pi_{ph,4}^*(a_2)$	38					
Q_3 (A_1)	$\pi_3(a_2) \rightarrow \sigma^*(b_1)$	52	3.64	341	-	3.27	Diss
	$\pi_2(b_2) \rightarrow \sigma^*(a_1)$	15					
	$\pi_2(b_2) \rightarrow \sigma^*(b_1)$	11					
Q_4 (A_1)	$\pi_{ph,2}(b_1) \rightarrow \pi_{ph,4}^*(a_2)$	81	4.68	265	-	3.47	Intra Ph
	$\pi_{ph,3}(a_2) \rightarrow \pi_{ph,5}^*(b_1)$	17					
Q_5 (B_2)	$\pi_{ph,3}(a_2) \rightarrow \pi_{ph,4}^*(a_2)$	60	4.73	262	-	3.46	Intra Ph
	$\pi_{ph,2}(b_1) \rightarrow \pi_{ph,5}^*(b_1)$	37					

Table S5. Vertical excitation energies (E), wavelengths (λ), oscillator strengths (f), and singly-excited configurations of the main excited doublet-doublet and doublet-quartet transitions involved in the initial absorption of $^2\mathbf{1}^{-1}$ within the Franck-Condon region. Calculated at the MS-RASPT2 level of theory using RAS_{Diss} and a level shift of 0.3 a.u.

	Transition	Weight / %	E / eV	λ / nm	f	Character
D_0 (B_2)	HF	83	-	-	-	HF
D_1 (A_1)	$\pi_4^*(b_2) \rightarrow \sigma^*(a_1)$	70	2.58	480	0.0001	Diss
D_2 (A_2)	$\pi_3(a_2) \rightarrow \pi_4^*(b_2)$	47	2.63	471	0.2630	HOMO $\rightarrow$ LUMO
	$\pi_2(a_2) \rightarrow \pi_4^*(b_2)$	30				HOMO-1 $\rightarrow$ LUMO
D_3 (B_1)	$\pi_4^*(b_2) \rightarrow \sigma^*(b_1)$	73	2.83	438	0.0000	Diss
D_4 (A_2)	$\pi_2(a_2) \rightarrow \pi_4^*(b_2)$	46	3.44	360	0.0006	HOMO-1 $\rightarrow$ LUMO
	$\pi_3(a_2) \rightarrow \pi_4^*(b_2)$	32				HOMO $\rightarrow$ LUMO
D_5 (B_1)	$\pi_4^*(b_2) \rightarrow \pi_{ph,5}^*(b_1)$	86	3.64	341	0.0000	CT
D_6 (A_1)	$\pi_3(a_2) \rightarrow \sigma^*(b_1)$	54	4.61	269	0.0009	Diss
Q_1 (B_1)	$\pi_3(a_2) \rightarrow \sigma^*(a_1)$	58	4.26	291	-	Diss
	$\pi_2(a_2) \rightarrow \sigma^*(a_1)$	17				
Q_2 (A_1)	$\pi_3(a_2) \rightarrow \sigma^*(b_1)$	55	4.43	280	-	Diss
	$\pi_2(a_2) \rightarrow \sigma^*(b_1)$	18				
Q_3 (B_1)	$\pi_2(b_2) \rightarrow \sigma^*(a_1)$	48	4.96	250	-	Diss
	$\pi_3(a_2) \rightarrow \sigma^*(a_1)$	21				
	$\pi_2(b_2) \rightarrow \sigma^*(b_1)$	11				
Q_4 (A_1)	$\pi_2(a_2) \rightarrow \sigma^*(b_1)$	45	5.13	242	-	Diss
	$\pi_3(a_2) \rightarrow \sigma^*(b_1)$	23				
	$\pi_2(b_2) \rightarrow \sigma^*(a_1)$	11				

Table S6. Vertical excitation energies (E), wavelengths (λ), oscillator strengths (f), and singly-excited configurations of the main excited doublet-doublet and doublet-quartet transitions involved in the initial absorption of $^2\mathbf{1}^{-1}$ within the Franck-Condon region. Calculated at the MS-RASPT2 level of theory using RAS$_{CT}$ and a level shift of 0.3 a.u.

	Transition	Weight / %	E / eV	λ / nm	f	Character
D_0 (B$_2$)	HF	81	-	-	-	HF
D_1 (B$_1$)	$\pi_4^*(b_2) \rightarrow \pi_{ph,5}^*(b_1)$	83	2.11	587	0.0000	CT
D_2 (A$_2$)	$\pi_3(a_2) \rightarrow \pi_4^*(b_2)$	72	2.49	497	0.1831	HOMO $\rightarrow$ LUMO
D_3 (B$_1$)	$\pi_4^*(b_2) \rightarrow \sigma^*(b_1)$	67	3.03	409	0.0000	Diss
D_4 (A$_2$)	$\pi_2(a_2) \rightarrow \pi_4^*(b_2)$	66	3.35	370	0.0101	HOMO-1 $\rightarrow$ LUMO
D_5 (A$_2$)	$\pi_4^*(b_2) \rightarrow \pi_4^*(a_2)$	38	3.54	350	0.1503	CT
	$\pi_4^*(b_2) \rightarrow \pi_{ph,5}^*(b_1)$	29				
D_6 (A$_2$)	$\pi_4^*(b_2) \rightarrow \pi_{ph,4}^*(a_2)$	50	4.36	284	0.1501	CT
	$\pi_4^*(b_2) \rightarrow \pi_4^*(a_2)$	23				
Q_1 (B$_2$)	$\pi_{ph,3}(a_2) \rightarrow \pi_{ph,4}^*(a_2)$	60	4.38	283	-	Intra Ph
	$\pi_{ph,2}(b_1) \rightarrow \pi_{ph,5}^*(b_1)$	23				
Q_2 (A$_1$)	$\pi_3(a_2) \rightarrow \pi_{ph,5}^*(b_1)$	82	4.72	262	-	Intra Ph
Q_3 (B$_1$)	$\pi_3(a_2) \rightarrow \sigma^*(a_1)$	34	4.89	254	-	Diss
	$\pi_2(a_2) \rightarrow \sigma^*(a_1)$	23				
	$\pi_2(b_2) \rightarrow \sigma^*(b_1)$	13				
Q_4 (A$_1$)	$\pi_{ph,3}(a_2) \rightarrow \pi_{ph,5}^*(b_1)$	41	5.06	245	-	Intra Ph
	$\pi_{ph,2}(b_1) \rightarrow \pi_{ph,4}^*(a_2)$	39				
Q_5 (B$_2$)	$\pi_{ph,2}(b_1) \rightarrow \pi_{ph,5}^*(b_1)$	57	5.23	237		Intra Ph
	$\pi_{ph,3}(a_2) \rightarrow \pi_{ph,4}^*(a_2)$	20				

2. Light-induced charging of the PS

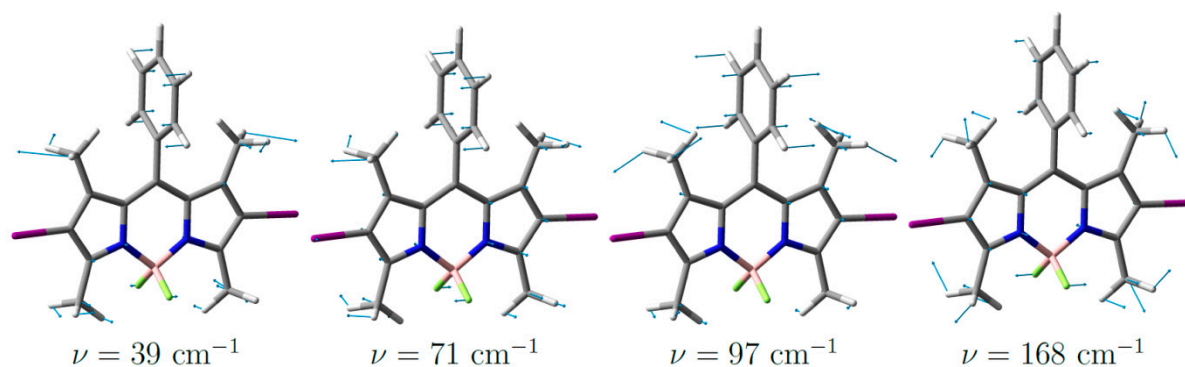**Table S7.** SOC between the bright S_1 and CT states. Calculated at the MS-RASPT2 level of theory using RAS_{CT} in $^1\mathbf{1}^0$ geometry.

	Transition	E / eV	Character	SOC with S_1 / cm^{-1}
T_1 (B_1)	$\pi_3(a_2) \rightarrow \pi_4^*(b_2)$	1.90	HOMO $\rightarrow$ LUMO	-
T_2 (B_1)	$\pi_2(a_2) \rightarrow \pi_4^*(b_2)$	3.04	HOMO-1 $\rightarrow$ LUMO	-
T_7 (A_2)	$\pi_{ph,2}(b_2) \rightarrow \pi_4^*(b_2)$	4.93	CT	5.3
T_8 (B_1)	$\pi_{ph,3}(a_2) \rightarrow \pi_4^*(b_2)$	5.09	CT	-
T_{10} (B_2)	$\pi_3(a_2) \rightarrow \pi_{ph,5}^*(b_1)$	5.51	CT	0.0
T_{11} (A_1)	$\pi_3(a_2) \rightarrow \pi_{ph,4}^*(a_2)$	5.52	CT	0.5

$\nu = 45$ cm^{-1} $\nu = 71$ cm^{-1} $\nu = 102$ cm^{-1} $\nu = 170$ cm^{-1}
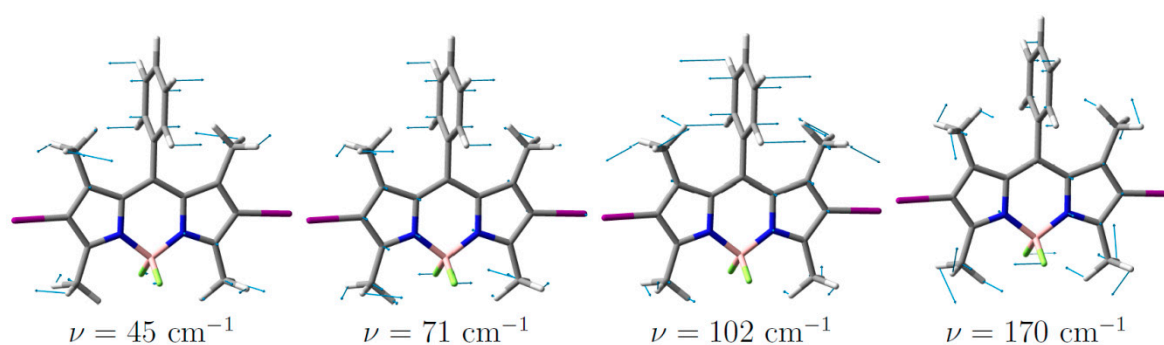
Figure S3. Vibrational modes at GS geometry $^1\mathbf{1}^0$ corresponding to a torsion around the main/side ring dihedral.

Table S8. SOC for $^1\mathbf{1}^0$ at a torsion of 55° (C_2 symmetry) obtained by RASPT2 with RAS_{CT} and a level shift of 0.3 a.u.

|	Transition	E / eV	Character	SOC with S_1 / cm^{-1}
S_1 (B)	$\pi_3(a) \rightarrow \pi_4^*(b)$	2.68	HOMO $\rightarrow$ LUMO	-
T_1 (B)	$\pi_3(a) \rightarrow \pi_4^*(b)$	0.90	HOMO $\rightarrow$ LUMO	0.1
T_2 (B)	$\pi_2(a) \rightarrow \pi_4^*(b)$	2.03	HOMO-1 $\rightarrow$ LUMO	0.4
T_3 (A)	$\pi_{ph,2}(b) \rightarrow \pi_4^*(b)$	3.62	CT	4.0

Figure S4. Vibrational modes at GS geometry $^2\mathbf{1}^{-1}$ corresponding to a torsion around the main/side ring dihedral.

Table S9. SOC between the bright S_1 and dissociative states. Calculated at the MS-RASPT2 level of theory using RAS$_{Diss}$ in $^1\mathbf{1}^0$ geometry.

|	Transition	E / eV	Character	SOC with S_1 / cm^{-1}
T_1 (B$_1$)	$\pi_3(a_2) \to \pi_4^*(b_2)$	1.88	HOMO $\to$ LUMO	-
T_2 (B$_1$)	$\pi_2(a_2) \to \pi_4^*(b_2)$	3.02	HOMO-1 $\to$ LUMO	-
T_5 (A$_2$)	$\pi_3(a_2) \to \sigma^*(a_1)$	4.78	Diss	0.6
T_6 (B$_2$)	$\pi_3(a_2) \to \sigma^*(b_1)$	5.06	Diss	39.2

3. Photo-degradation
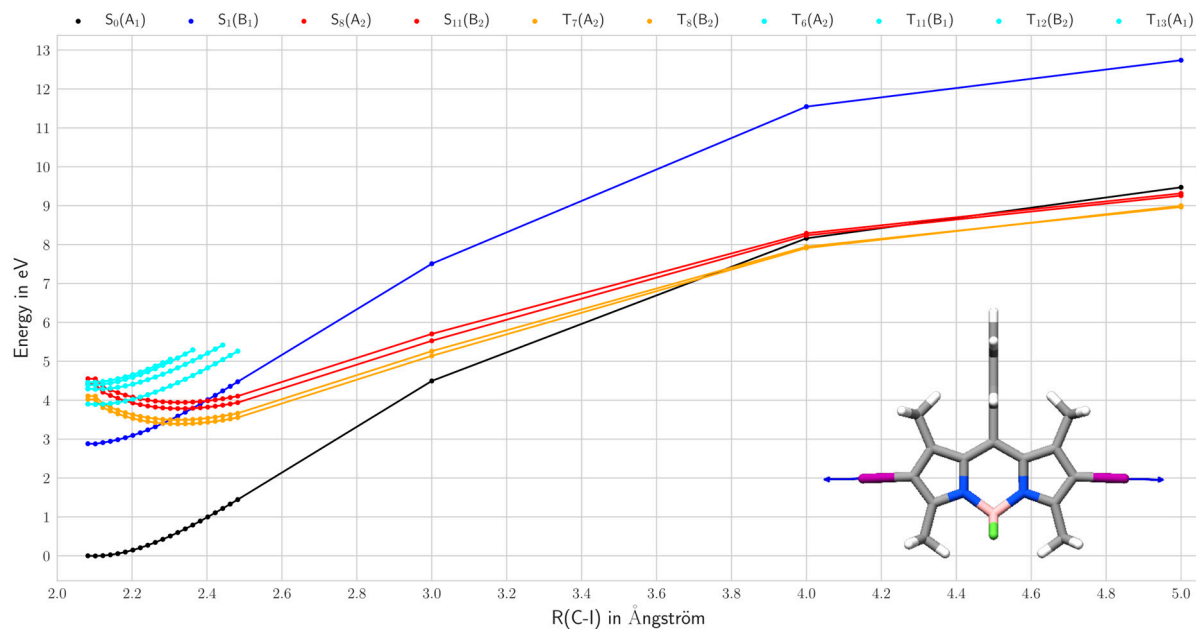
Figure S5. TDDFT PESs along the doubly dissociative (C-I) coordinate for the non-reduced dye. No dissociative behaviour can be observed. Colour code: singlet ground state (black), excited singlet state (blue), dissociative singlet state (red), triplet state (green), dissociative triplet state (orange), triplet CT state (cyan).
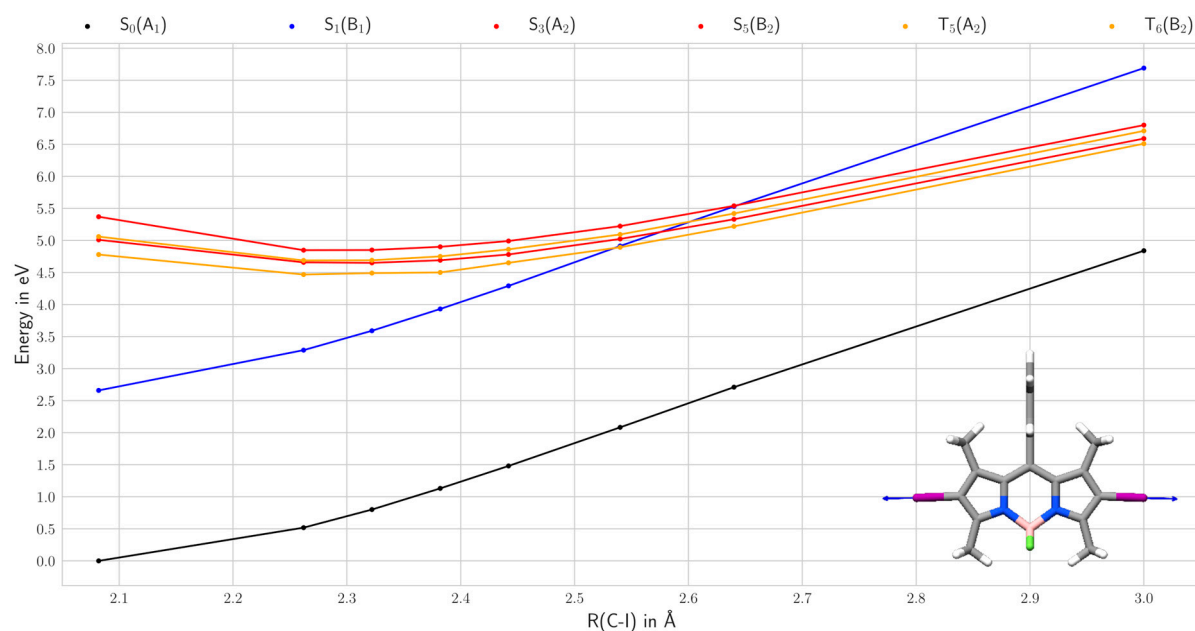
Figure S6. PESs along the unrelaxed doubly dissociative (C-I) coordinate for the non-reduced dye. These potentials were calculated at the MS-RASPT2 level of theory using RAS_Diss and a level shift of 0.1 a.u. The unrelaxed coordinate was chosen to maintain the C_{2v} symmetry and thus reduce the computational costs. The reported energetic shift between RASPT2 and TDDFT can best be seen through the shift of the crossing point between S_1 and the dissociative states towards higher excitation energies and longer elongations compared to the TDDFT results in Figure S5. Colour code: singlet ground state (black), excited singlet state (blue), dissociative singlet state (red), triplet state (green), dissociative triplet state (orange).
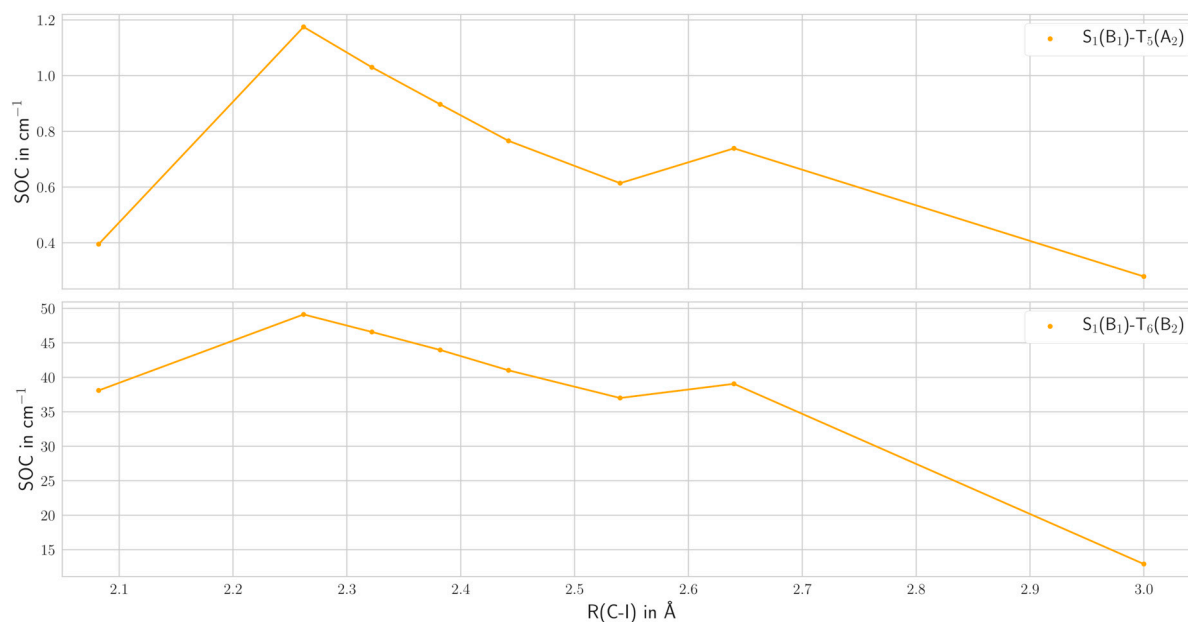
Figure S7. SOCs for the diabatic potentials along the unrelaxed doubly dissociative (C-I) coordinate between the $S_1(B_1)$ state and the two dissociative triplet states, $T_5(A_2)$ (above) and $T_6(B_2)$ (below); calculated at the MS-RASPT2 level of theory using RAS_Diss.
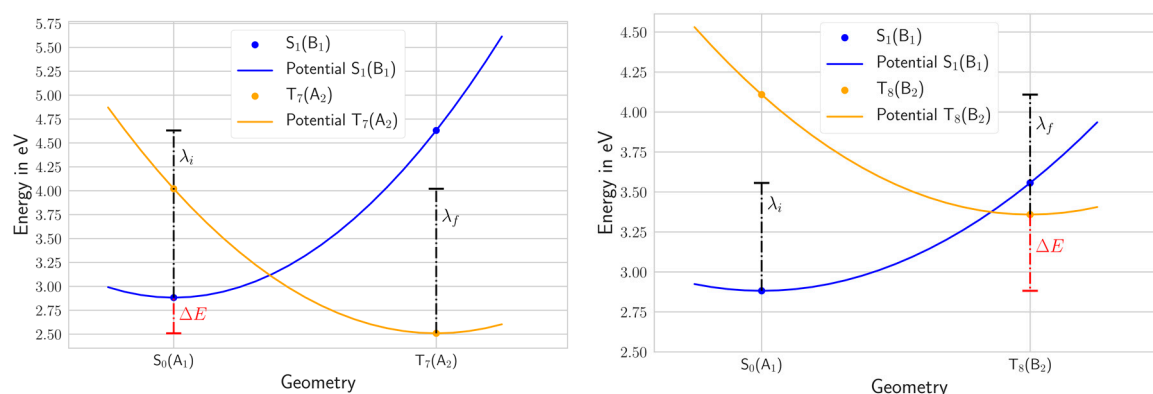
Figure S8. Quadratic potentials according to Marcus theory with energy difference (ΔE), and reorganization energy for initial (λ_i) and final (λ_f) geometry. Left: For an ISC from S_1 at GS geometry $^1\mathbf{1^0}$ to T_7 at its excited state geometry; mono-dissociation. Right: For an ISC from S_1 at GS geometry $^1\mathbf{1^0}$ to T_8 at its excited state geometry; di-dissociation.

Table S10. Results for ISC between S_1 / T_7 and S_1 / T_8 based on Marcus theory and Equation 1. f = final and i = initial, representing the geometry from which the reorganization energy was taken.

S_1 (B_1)	to $T_7(A_2)$	to $T_8(B_2)$
ΔE / eV	−0.37	0.48
λ(f) / eV	1.75	0.67
λ(i) / eV	1.51	0.75
SOC / cm^{-1}	0.58	39.22
t_{ISC}(f) / s	5.63×10^4	4.19×10^4
t_{ISC}(i) / s	5.92×10^5	6.62×10^4
k_{ISC}(f) / s^{-1}	1.78×10^3	2.39×10^3
k_{ISC}(i) / s^{-1}	1.69×10^4	1.51×10^3

Table S11. SOCs at the geometry derived from the crossing point of the S_1 and T_8 potentials obtained by RASPT2 with RAS$_{Diss}$ and a level shift of 0.3 a.u.

	Transition	E / eV	Character	SOC with S_1 / cm^{-1}
S_1 (B_1)	$\pi_3(a) \rightarrow \pi_4^*(b)$	2.72	HOMO $\rightarrow$ LUMO	-
T_5 (A_2)	$\pi_3(a_2) \rightarrow \sigma^*(a_1)$	3.72	Diss	1.7
T_6 (B_2)	$\pi_3(a_2) \rightarrow \sigma^*(b_1)$	3.91	Diss	53.0